

# 21st century projections of surface mass balance changes for major drainage systems of the Greenland ice sheet

M Tedesco<sup>1</sup> and X Fettweis<sup>2</sup>

<sup>1</sup> The City College of New York, 160 Convent Avenue, Marshak Building, Room J106, NY 10031, USA

<sup>2</sup> Department of Geography, University of Liège, Laboratory of Climatology (Bâtiment B11), Allée du 6 Août, 2, B-4000 Liège, Belgium

E-mail: [mtedesco@ccny.cuny.edu](mailto:mtedesco@ccny.cuny.edu)

Received 30 July 2012

Accepted for publication 11 October 2012


Published 8 November 2012

Online at [stacks.iop.org/ERL/7/045405](http://stacks.iop.org/ERL/7/045405)

## Abstract

Outputs from the regional climate model Modèle Atmosphérique Régionale at a spatial resolution of 25 km are used to study 21st century projected surface mass balance (SMB) over six major drainage basins of the Greenland ice sheet (GrIS). The regional model is forced with the outputs of three different Earth System Models (CanESM2, NorESM1 and MIROC5) obtained when considering two greenhouse gas future scenarios with levels of CO<sub>2</sub> equivalent of, respectively, 850 and >1370 ppm by 2100. Results indicate that the increase in runoff due to warming will exceed the increased precipitation deriving from the increase in evaporation for all basins, with the amount of net loss of mass at the surface varying spatially. Basins along the southwest and north coast are projected to have the highest sensitivity of SMB to increasing temperatures. For these basins, the global temperature anomaly corresponding to a decrease of the SMB below the 1980–99 average (when the ice sheet was near the equilibrium) ranges between +0.60 and +2.16 °C. For the basins along the northwest and northeast, these values range between +1.50 and +3.40 °C. Our results are conservative as they do not account for ice dynamics and changes in the ice sheet topography.

**Keywords:** Greenland, surface mass balance, future projections, sea level rise

 Online supplementary data available from [stacks.iop.org/ERL/7/045405/mmedia](http://stacks.iop.org/ERL/7/045405/mmedia)

## 1. Introduction and rationale

The Greenland ice sheet (GrIS) plays a crucial role in current estimates and future projections of sea level rise, highlighted by the recently observed response of polar ice to increasing surface temperatures (Lemke *et al* 2007, Comiso 2002, Abdalati and Steffen 2001, Serreze *et al* 2000, Vaughan and Doake 1996, Tedesco 2007, Tedesco *et al* 2008, 2011, Rignot *et al* 2004, 2011). The surface mass balance (SMB) of the GrIS can be approximated as the mass gained from solid accumulation minus the mass lost from meltwater runoff, with evaporation and sublimation being negligible (e.g., Box *et al* 2004). The effect of rising surface temperature on

the SMB can be twofold: on one hand, it can decrease SMB through enhanced surface melting and runoff; on the other hand, a warmer climate may be also responsible for increasing atmospheric moisture content, leading to increased solid accumulation and potentially pointing towards an increased SMB. Recent surface melting records studied by means of remote sensing data and modelling outputs indicate increasing runoff along the west coast of Greenland (Tedesco 2007, Tedesco *et al* 2008, 2011, Fettweis *et al* 2011) and measurements performed in the interior of Greenland indicate thickening in its interior (Krabill *et al* 2000, Thomas *et al* 2001) while the thickening rate is observation dependent (Thomas *et al* 2006).

In this context, studying how SMB, runoff and accumulation will be affected by a warming climate is key to understanding and quantifying the future behaviour of the GrIS. In particular, because of the diverse response to warming expected from different areas of the GrIS (e.g., depending on topography, atmospheric circulation and latitudinal gradient, for example), it is essential to study SMB trends at a regional scale. Moreover, a detailed spatial representation of the response of the GrIS to a warming climate is the basis for the coupling of surface ice sheet hydrology models with surface mass balance models, with the overall goal of reducing uncertainties associated with projections of the total mass balance (Alley and Joughin 2012, Helsen *et al* 2012).

General Circulation Models (GCMs) and Earth System Models (ESMs) generate global scale projections of (near-surface) temperature and other variables driving SMB, but at a relatively coarse spatial resolution. This limits their use in studying the spatio-temporal evolution of the SMB over the GrIS, where the ablation zone width (e.g., the area where runoff exceeds accumulation) in many places is of the order of magnitude of the spatial resolution of the GCMs outputs. Moreover, many of the GCMs or ESMs often use a simplistic parameterization to describe the physical processes used to obtain parameters related to the SMB. Compared to GCMs, regional climate models (RCMs) are computationally more expensive but produce physically based outputs at a higher spatial resolution.

The combination of GCMs and RCMs offer a unique opportunity to project SMB changes over the GrIS at high spatial resolution. Outputs from GCMs can, indeed, be used to generate forcings for regional models, which, because of their higher resolution and more detailed physics, can generate the required outputs for a more appropriate regional SMB analysis. In this study, we force the Modèle Atmosphérique Régionale (MAR) regional model (e.g., Fettweis *et al* 2011 and Tedesco *et al* 2011) with the outputs of three different ESMs from the Coupled Model Intercomparison Project Phase 5 (CMIP5) database obtained considering two recommended radiative forcing scenarios (Moss *et al* 2010), planned to be used in the next report of the Intergovernmental Panel on Climate Change (IPCC). One of the advantages of MAR over most other available RCMs is that it incorporates a sophisticated snow model (Brun *et al* 1992) and thus actually calculates all SMB components. Moreover, the availability of the MAR outputs at a spatial resolution of 25 km allows for the study of SMB projections at a regional scale. In particular, we divide the GrIS into six drainage basins (figure 1) based on topography. For each basin, we study the annual near-surface air temperature (3 m, TAS), the SMB and the relative driving components (e.g., runoff, snowfall, rainfall) obtained from MAR when forced with the outputs of the ESMs. We compare the TAS and SMB changes at basin scale with those of globally averaged TAS anomalies obtained by the ESMs. Our main goals consist of evaluating the SMB projections for the 21st century over the different drainage systems; studying the sensitivity of TAS and SMB of each of the drainage basins to TAS global ESM anomalies; and identifying TAS global ESM

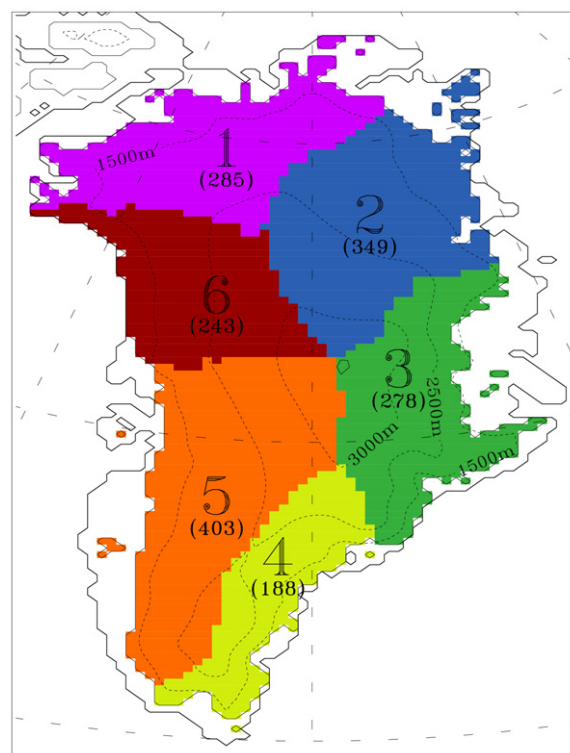


**Figure 1.** Map of the Greenland ice sheet drainage basins used in this study. Numbers in parentheses indicate the area of each basin in thousands of square kilometres.

anomaly values for which the SMB of each would fall below the mean SMB values during the historical period (1980–99).

## 2. Models and scenarios

For studying the current climate, the ERA-40 reanalysis (1958–78) and after that the ERA-INTERIM reanalysis (1979–2011) from the European Centre for Medium Range Weather Forecasts (ECMWF) are used to initialize the meteorological fields at the beginning of the MAR simulation in September 1957 and to force the MAR lateral boundaries with temperature, specific humidity and wind components every 6 h during the simulation. The sea surface temperature (SST) and the sea ice cover (SIC) are also prescribed by the reanalysis. The atmospheric model within MAR interacts with a physically based snow/ice model (Brun *et al* 1992), which provides the state of the snowpack and associated quantities (e.g., runoff, liquid water content, etc). We refer to Fettweis *et al* (2012) for a more detailed description of the MAR version used here as well as its setup. The outputs of the MAR model over Greenland have been evaluated in several studies (e.g., Lefebvre *et al* 2005 and Fettweis *et al* 2005). Recently, Fettweis *et al* (2011) have assessed the outputs of the MAR model using automatic weather station measurements and melt time series derived from passive microwave data. Box *et al* (2012) also evaluated MAR downward shortwave (SW) radiation and surface temperature (2001–10) against *in situ* weather station data from the Greenland Climate Network (GC-Net).

**Table 1.** Linear regression coefficients between MAR regional and ESM mean global-surface temperature anomalies (2006–2010). Numbers in the parentheses indicate the coefficient of determination ( $R^2$ ). The last two columns report the multi-model mean ( $\mu$ ) of the RCP45 and RCP85 simulations, as well as the standard deviation ( $\sigma$ ).

Basin	NorESM1		CanESM2		MIROC5		Multi-model	Multi-model
	RCP45	RCP85	RCP45	RCP85	RCP45	RCP85	$\mu_{\text{RCP45}} \pm \sigma_{\text{RCP45}}$	$\mu_{\text{RCP85}} \pm \sigma_{\text{RCP85}}$
1	1.55 (0.65)	1.41 (0.85)	1.67 (0.83)	1.57 (0.93)	1.28 (0.57)	1.65 (0.87)	$1.50 \pm 0.20$	$1.55 \pm 0.12$
2	1.45 (0.63)	1.34 (0.87)	1.67 (0.83)	1.52 (0.92)	1.10 (0.52)	1.53 (0.85)	$1.41 \pm 0.29$	$1.46 \pm 0.10$
3	1.30 (0.59)	1.22 (0.84)	1.47 (0.77)	1.28 (0.89)	0.92 (0.43)	1.34 (0.84)	$1.23 \pm 0.28$	$1.28 \pm 0.06$
4	1.30 (0.61)	1.21 (0.82)	1.36 (0.74)	1.16 (0.88)	0.78 (0.38)	1.20 (0.82)	$1.15 \pm 0.32$	$1.19 \pm 0.03$
5	1.23 (0.50)	1.20 (0.78)	1.42 (0.70)	1.20 (0.86)	0.82 (0.33)	1.23 (0.78)	$1.16 \pm 0.31$	$1.21 \pm 0.02$
6	1.31 (0.52)	1.24 (0.79)	1.51 (0.73)	1.31 (0.88)	0.99 (0.40)	1.37 (0.79)	$1.27 \pm 0.26$	$1.31 \pm 0.06$

The three ESMs used in this study to generate the forcing over 1980–2100 for MAR are the Norwegian Community Earth System Model (NorESM1), the second generation of the Canadian Earth System Model (CanESM2) and the Model for Interdisciplinary Research on Climate (MIROC5) of the University of Tokyo, Japan. The ESMs are used to generate MAR outputs for the historical period (1980–2005) and for future projections (2005–2100). The Canadian Earth System Model (CanESM2, e.g. Arora and Boer 2010 and Chylek *et al* 2011) combines the fourth generation climate model (CanCM4) from the Canadian Center for Climate Modelling and Analysis model with the terrestrial carbon cycle based on the Canadian Terrestrial Ecosystem Model (CTEM), which models the land–atmosphere carbon exchange. The Norwegian community Earth System Model (NorESM1) is built under the structure of the Community Earth System Model (CESM) from the National Center for Atmospheric Research (NCAR). The major difference from the standard CESM configuration concerns the modification of the treatment of atmospheric chemistry, aerosols and clouds (Seland *et al* 2008), and the ocean component. Lastly, the Model for Interdisciplinary Research on Climate (MIROC) is a coupled general circulation model developed at the Center for Climate System Research (CCSR) of the University of Tokyo, composed of the CCSR/NIES (National Institute of Environmental Studies) atmospheric general circulation model (AGCM 5.5) and the CCSR Ocean Component Model, including a dynamic–thermodynamic sea ice model (e.g., Watanabe *et al* 2010, 2011). The three models have been chosen in Fettweis *et al* (2012) among the CMIP5 ESMs because of their ability to simulate the current climate (general circulation and summer atmospheric temperature at 700 hPa) over Greenland. In particular, MAR forced by these three ESMs performs satisfactorily over the period 1980–99 with respect to MAR forced by ERA-INTERIM, with most of the biases being below the inter-annual variability of MAR forced by ERA-INTERIM. We refer to Fettweis *et al* (2012) for the evaluation of the outputs of MAR when forced with the outputs of the ESMs during the historical period (1980–2005).

The first of the two CO<sub>2</sub> future scenarios considered in this study (denoted as RCP45) corresponds to an increase of the atmospheric greenhouse gas concentration to a level of 850 ppm CO<sub>2</sub> equivalent by 2100. The second scenario (RCP85) corresponds to an increase of the atmospheric greenhouse gas concentration to a level of >1370 ppm

CO<sub>2</sub> equivalent by 2100. More detailed information on the scenarios can be found in Moss *et al* (2010) or Meinshausen *et al* (2011).

### 3. Results and discussion

We point out that the discussion reported in the following is based on the analysis of annual values of the quantities under study smoothed using a 30 yr filter, unless stated otherwise. A 30 yr running mean was applied to the time series to remove the inter-annual variability and to improve the readability of the figures. Using a filter based on a shorter period (e.g. 10 yr) did not considerably impact the results. We also point out that both SMB and TAS changes over the 21st century are given with respect to the 1980–99 average.

#### 3.1. Near-surface temperature

Figure 2 illustrates the regionally averaged TAS anomaly obtained from MAR (when forced with the two RCP scenarios and ESMs outputs) as a function of TAS global anomaly values from the ESMs computed over 1980–2100, using the period 1980–99 as a baseline after having applied a 30 yr running mean. We point out that, in view of the physically based nature of the coupled atmosphere/snow model in MAR, the TAS anomaly projected by the model for each basin accounts for the impact on TAS of the different terms of the surface energy balance (e.g., albedo, latent heat and surface heat fluxes, etc). In table 1, we report the linear regression coefficients relating the TAS from MAR to global ones. The number in the parentheses in the table represent the coefficient of determination ( $R^2$ ), defined as the square of the correlation coefficient between the outcomes and their predicted values. The simulations obtained with MIROC5-RCP45 for Basins 3–6 are the only ones where the regression coefficients are below 1, with values ranging between 0.78 and 0.99, with relatively low values of the coefficient of determination (0.3–0.4). The coefficients for the remaining simulations are above 1 for all basins. This implies that the projected warming over the GrIS is higher than the global warming, as a consequence of the Arctic amplification already pointed out over current climate by Serreze *et al* (2009), with the exception of the MIROC5-RCP45 forced MAR simulation. The regression

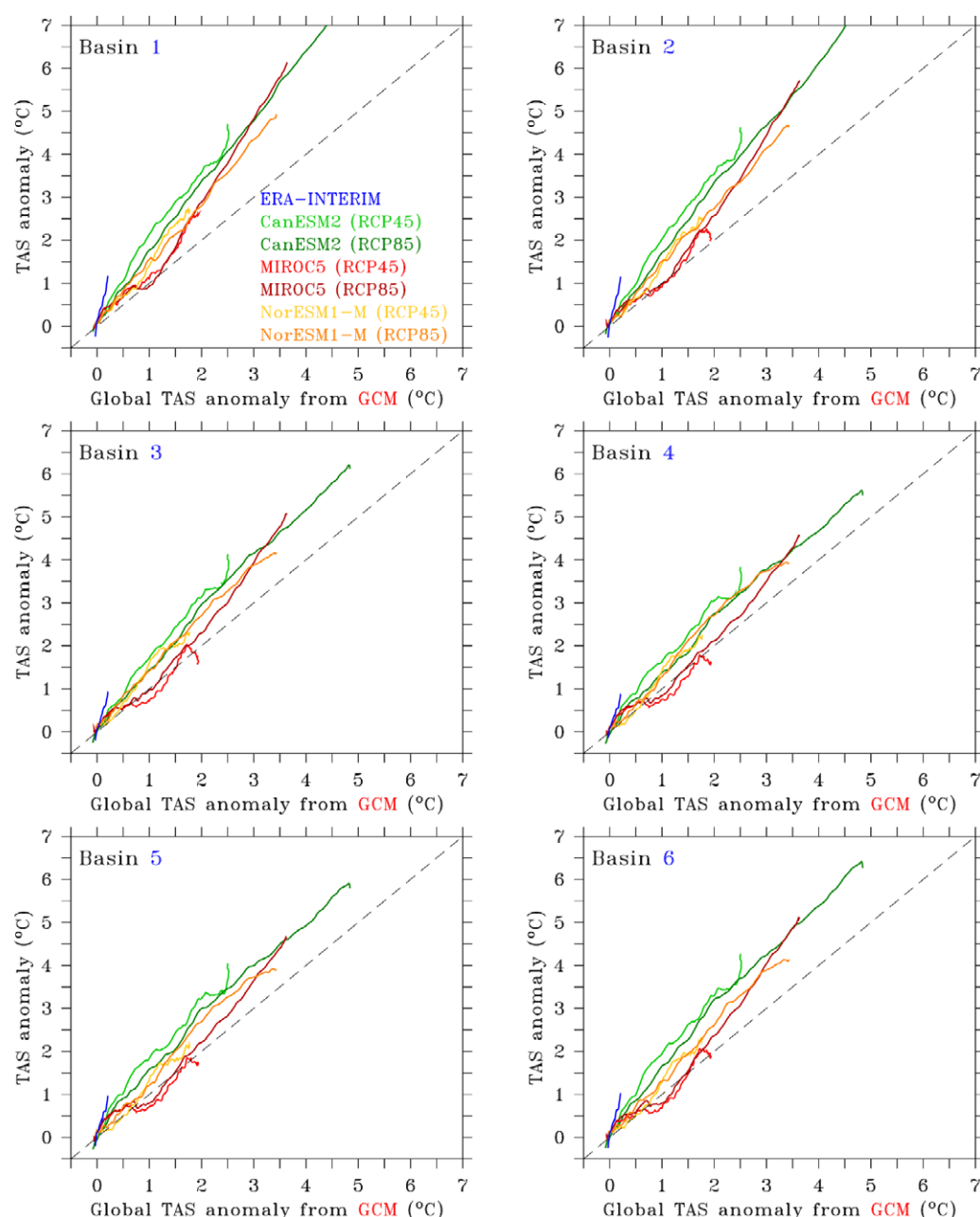


**Figure 2.** MAR basin-averaged surface (3 m) temperature anomaly values (1980–99 baseline) from the different simulations as a function of the global mean surface temperature anomaly obtained from the ESM used to force MAR. For readability purposes, a 30 yr running mean was applied to the data in the plots.

coefficients for the multi-model mean in the case of the two  $\text{CO}_2$  scenarios (obtained from the average of the regression coefficients for the different simulations) and the corresponding standard deviations are also reported in table 1. The coefficients for the multi-model mean are similar for all basins, for both  $\text{CO}_2$  scenarios. The results obtained with the RCP45 scenario, however, show a higher value of standard deviation than those obtained with the RCP85 scenario, because the temperature changes in the case of RCP45 are lower than those in the case of RCP85, with the results less driven by the ESM dependent inter-annual variability. The highest model-averaged regression coefficients are obtained

for the north (Basin 1) and northeast (Basin 2) basins, with values ranging between  $1.41 \pm 0.29$  and  $1.55 \pm 0.12$ . This might be the consequence of the local warming induced by the Arctic sea ice cover reduction (Fettweis *et al* 2012). Basins 3 (east) and 6 (northwest) have also similar regression coefficients for the multi-model mean, with their values ranging between  $1.23 \pm 0.28$  and  $1.31 \pm 0.06$ . Lastly, the remaining Basins 4 and 5 are the ones with the lowest-averaged coefficients, with values between  $1.15 \pm 0.32$  and  $1.21 \pm 0.02$ , because the temperature increase over these basins is dampened by the thermal inertia of the Atlantic Ocean. The warming is generally higher for the remaining



**Table 2.** Mean SMB values and standard deviation for the period 1980–99 obtained from MAR when forced with ERA-INTERIM and the outputs of the three ESM models.

1980–99 SMB values (Gt yr <sup>-1</sup> )								
Basin	ERA-INTERIM		NorESM1		CanESM2		MIROC5	
	$\mu$	$\sigma$	$\mu$	$\sigma$	$\mu$	$\sigma$	$\mu$	$\sigma$
1	22	17	54	16	-2	23	14	22
2	40	13	56	18	59	14	31	18
3	114	27	105	23	134	26	112	24
4	116	19	117	30	154	22	149	25
5	58	46	93	38	74	48	82	41
6	39	18	58	24	-9	20	48	19

basins as they are more affected by the sea ice cover decrease than Basins 4 and 5, which are already surrounded by open water for most of the year.

### 3.2. SMB over current climate

Before discussing the projected SMB trends over the drainage basins, in this section we analyse the SMB over current climate obtained by MAR when forced with ERA-INTERIM with respect to the same quantity simulated by the three ESMs (table 2). This analysis is important because a low (high) SMB bias (with respect to ERA-INTERIM runs over 1980–99) can result in a slower (faster) rate of SMB decrease relative to other simulations, as a consequence of the fact that the melt does not increase linearly with temperature (Franco *et al* 2012). Results in table 2 indicate that CanESM2 overestimates SMB (with respect to the current climate values obtained with ERA-INTERIM,  $SMB_{ERA-1980-1999}$ ) in Basin 4 and underestimates SMB in Basins 1 and 6. Results from NorESM1 overestimate SMB over Basins 1 and 5 while MIROC5 overestimates SMB in Basin 5. In the remaining cases, all biases are below the inter-annual variability of the ERA-INTERIM forced MAR run. We refer to Fettweis *et al* (2012) for more explanations about these biases.

### 3.3. Future projections of SMB

The annual SMB anomalies (Gt yr<sup>-1</sup>) obtained from the different simulations over the different basins are plotted in figure 3 as a function of the ESM TAS global anomalies. A similar plot for runoff is reported in figure 4. In the supplementary material (available at [stacks.iop.org/ERL/7/045405/mmedia](http://stacks.iop.org/ERL/7/045405/mmedia)), for the reader's convenience, we also show the same plots for rainfall (figure S1 available at [stacks.iop.org/ERL/7/045405/mmedia](http://stacks.iop.org/ERL/7/045405/mmedia)), snowfall (figure S2 available at [stacks.iop.org/ERL/7/045405/mmedia](http://stacks.iop.org/ERL/7/045405/mmedia)), and albedo (figure S3 available at [stacks.iop.org/ERL/7/045405/mmedia](http://stacks.iop.org/ERL/7/045405/mmedia)). All simulations point to a negative SMB trend, indicating that the increase in runoff and rainfall will exceed the increase in snowfall. The projected increase for rainfall (figure S1 available at [stacks.iop.org/ERL/7/045405/mmedia](http://stacks.iop.org/ERL/7/045405/mmedia)) is generally smaller than the increase in snowfall (figure S2 available at [stacks.iop.org/ERL/7/045405/mmedia](http://stacks.iop.org/ERL/7/045405/mmedia)) for most basins, with the exception of Basins 4

and 5, where the increase in rainfall is greater than or comparable to the snowfall increase. In table 3 we report the values of the regression coefficients (and the coefficient of determination in the parentheses) between the SMB anomalies and ESM TAS global anomalies. In contrast to the case of the near-surface temperature analysis, the results from the two CO<sub>2</sub> scenarios suggest a different sensitivity of the SMB in each drainage basin to ESM TAS global anomalies, with the results obtained from the simulations using RCP85 showing higher regression coefficients than those obtained in the case of the RCP45 scenario. The MAR results discrepancies for a same RCP scenario are largely due to the ESMs sensitivity to the greenhouse gases scenarios considered, which propagate into the MAR outputs through the forcing applied at the boundaries of the MAR region containing Greenland. The basin with the highest multi-model-averaged regression coefficients is Basin 5 (thus the most sensitive to ESM TAS changes), in southwest Greenland, with a multi-model average trend of  $-40.59 \pm 8.39$  Gt yr<sup>-1</sup> °C<sup>-1</sup> in the case of the RCP45 scenario and  $-68.27 \pm 21.78$  Gt yr<sup>-1</sup> °C<sup>-1</sup> in the case of RCP85. For this basin, the maximum projected SMB, runoff, snowfall and rainfall anomalies are, respectively,  $\sim -250$  Gt yr<sup>-1</sup> (SMB),  $\sim +300$  Gt yr<sup>-1</sup> (runoff),  $+50$  Gt yr<sup>-1</sup> (snowfall) and  $+50$  Gt yr<sup>-1</sup> (rainfall), corresponding to a global near-surface temperature anomaly of  $\sim +3.5$  °C. This basin is strongly affected by southerly warm air advection because of the average general circulation flowing from southwest to northeast over Greenland. Moreover, Basin 5 is also the one with the highest projected runoff rate, given that the average surface temperature is already near the melting point over the current climate during the summer (June through August). For the same basin, the maximum projected decrease in albedo is about  $-0.1$  in the case of the CanESM2-RCP85 scenario (figure S3 available at [stacks.iop.org/ERL/7/045405/mmedia](http://stacks.iop.org/ERL/7/045405/mmedia)), because of the expansion of the bare ice zone (Franco *et al* 2012). Basin 1 in north Greenland ranks second in terms of sensitivity of SMB to ESM TAS global anomalies, with a regression coefficient for the multi-model average of  $-22.58 \pm 4.86$  Gt yr<sup>-1</sup> °C<sup>-1</sup> in the case of the RCP45 scenario and  $-38.99 \pm 9.92$  Gt yr<sup>-1</sup> °C<sup>-1</sup> in the case of the RCP85 scenario. For this basin, the maximum projected negative SMB anomaly is  $\sim -200$  Gt yr<sup>-1</sup> for a TAS global anomaly of  $\sim +5$  °C. For the same basin, the projected increase in rainfall is smaller than the projected increase in snowfall (see figures S1 and S2 available at [stacks.iop.org/ERL/7/045405/mmedia](http://stacks.iop.org/ERL/7/045405/mmedia)), with the SMB negative trend mostly driven by the projected increasing runoff. The projected albedo decrease for this basin suggests a maximum decrease similar to that of Basin 5 ( $\sim -0.1$ ), but occurring at a lower TAS global anomaly than that of Basin 5 ( $\sim +4$  °C in the case of Basin 1 versus a value of  $\sim +5$  °C in the case of the Basin 5). Multi-model-averaged trends for Basin 4 in southeast Greenland (ranking third in terms of sensitivity to global near-surface temperature anomaly) are  $-19.88 \pm 2.43$  Gt yr<sup>-1</sup> °C<sup>-1</sup> for the RCP45 scenario and  $35.50 \pm 4.57$  Gt yr<sup>-1</sup> °C<sup>-1</sup> in the case of the RCP85 scenario. For this basin, a large contribution of the increase to runoff

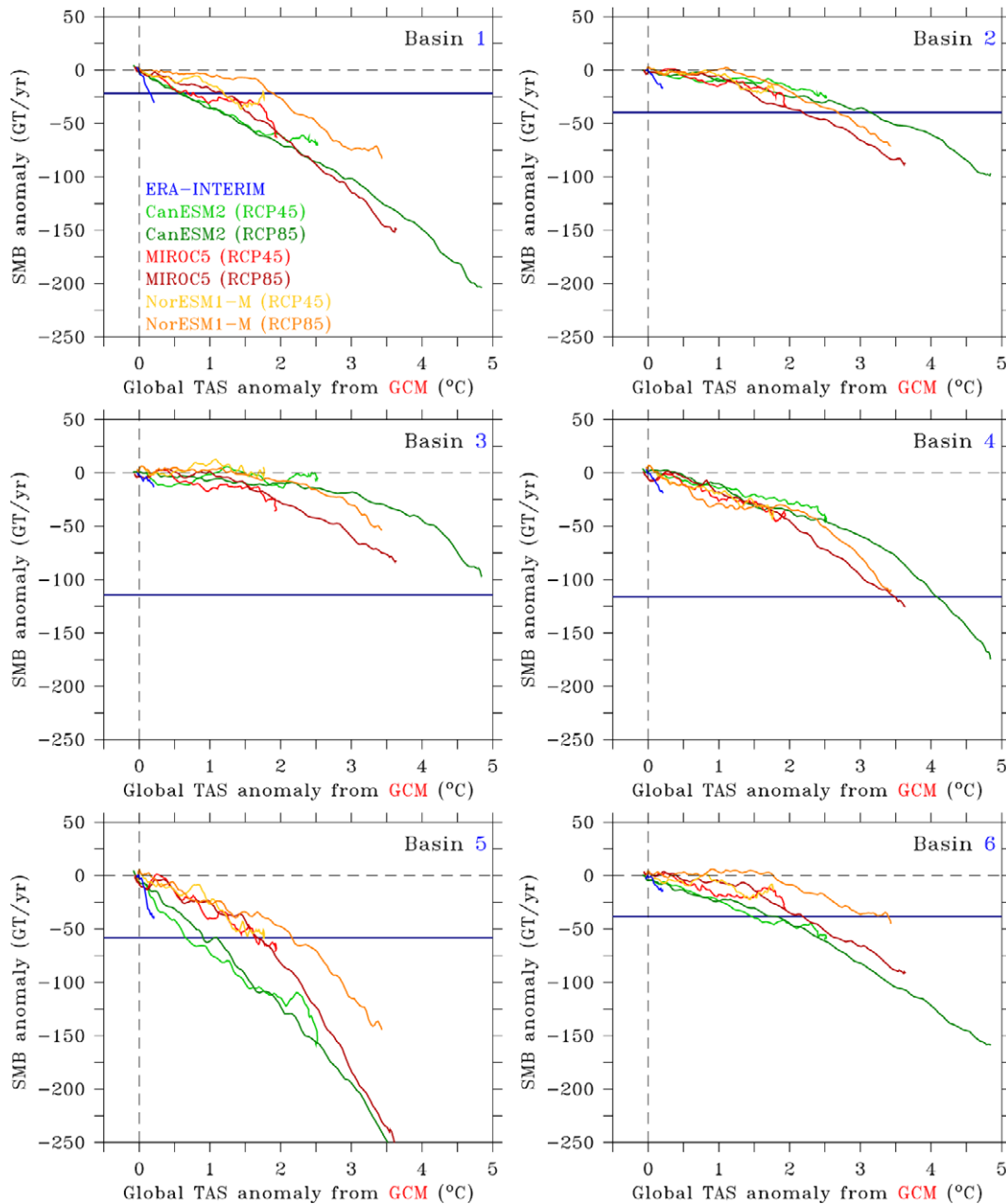


**Figure 3.** Same as figure 2 but for the SMB anomaly. Horizontal continuous lines indicate the SMB anomaly that will balance the basin-wide mean SMB for the period 1980–99 obtained from MAR forced with ERA-INTERIM.

(one third in the case of the maximum projected runoff increase with the CanESM2-RCP85 configuration) is due to the increase of rainfall (figure S1 available at [stacks.iop.org/ERL/7/045405/mmedia](http://stacks.iop.org/ERL/7/045405/mmedia)), with the changes in projected snowfall being negligible. Basins 2 in the northeast and 6 along the northwest show similar trends of SMB as a function of the global near-surface temperature anomaly, with values around  $-10 \text{ Gt yr}^{-1} \text{ }^{\circ}\text{C}^{-1}$  in the case of the RCP45 scenario and  $\sim -25 \text{ Gt yr}^{-1} \text{ }^{\circ}\text{C}^{-1}$  in the case of the RCP85 scenario. Basin 3, along east Greenland, shows the weakest sensitivity to global TAS anomaly in the case of the RCP45 scenario, with a multi-model-averaged regression coefficient of  $-6.03 \pm 8.36 \text{ Gt yr}^{-1} \text{ }^{\circ}\text{C}^{-1}$ . But in the case of the RCP85 scenario, the multi-model-averaged regression coefficient is

comparable to those obtained in the case of Basins 2 and 4. We point out that one reason that SMB trends differ between the RCP45 and RCP85 scenarios for Basin 3, aside from the sensitivity of runoff to surface temperature change, lies in different projections of changes in snowfall.

Absolute values of SMB from each simulation cannot be used to estimate when the SMB becomes negative, because for those simulations underestimating (overestimating) the current SMB, a negative SMB will occur earlier (or later, if ever) during the 21st century. Because of this, we use the SMB mean value (denoted  $\text{SMB}_{\text{ERA}_1980-1999}$  hereafter) for the period 1980–99 obtained from MAR-ERA-INTERIM as a reference. In particular, we focus on identifying those years when the modelled annual SMB anomaly

**Table 3.** Same as table 1 but with respect to SMB anomaly.

Basin	2006–2100 SMB trend ( $\text{Gt yr}^{-1} \text{ } ^\circ\text{C}^{-1}$ )					
	NorESM1		CanESM2		MIROC5	
	RCP45	RCP85	RCP45	RCP85	RCP45	RCP85
1	−17.14 (0.28)	−27.78 (0.89)	−24.06 (0.86)	−42.56 (0.97)	−26.54 (0.65)	−46.65 (0.98)
2	−12.75 (0.31)	−23.22 (0.84)	−9.90 (0.63)	−21.63 (0.90)	−15.16 (0.51)	−27.55 (0.95)
3	−2.33 (0.05)	−17.45 (0.66)	−0.15 (0.1)	−20.26 (0.68)	−15.60 (0.39)	−27.24 (0.93)
4	−21.63 (0.64)	−30.23 (0.76)	−17.10 (0.55)	−37.75 (0.92)	−20.91 (0.58)	−38.52 (0.96)
5	−35.38 (0.43)	−43.41 (0.89)	−50.28 (0.83)	−84.02 (0.97)	−36.12 (0.64)	−77.39 (0.94)
6	−7.79 (0.01)	−15.21 (0.77)	−21.3 (0.91)	−35.15 (0.98)	−11.29 (0.31)	−29.73 (0.96)
					Multi-model	
					$\mu_{\text{RCP45}} \pm \sigma_{\text{RCP45}}$	$\mu_{\text{RCP85}} \pm \sigma_{\text{RCP85}}$
					−22.58 $\pm$ 4.86	−38.99 $\pm$ 9.92
					−12.60 $\pm$ 2.63	−24.15 $\pm$ 3.04
					−6.03 $\pm$ 8.36	−21.65 $\pm$ 5.04
					−19.88 $\pm$ 2.43	−35.50 $\pm$ 4.57
					−40.59 $\pm$ 8.39	−68.27 $\pm$ 21.78
					−13.46 $\pm$ 7.00	−26.70 $\pm$ 10.31

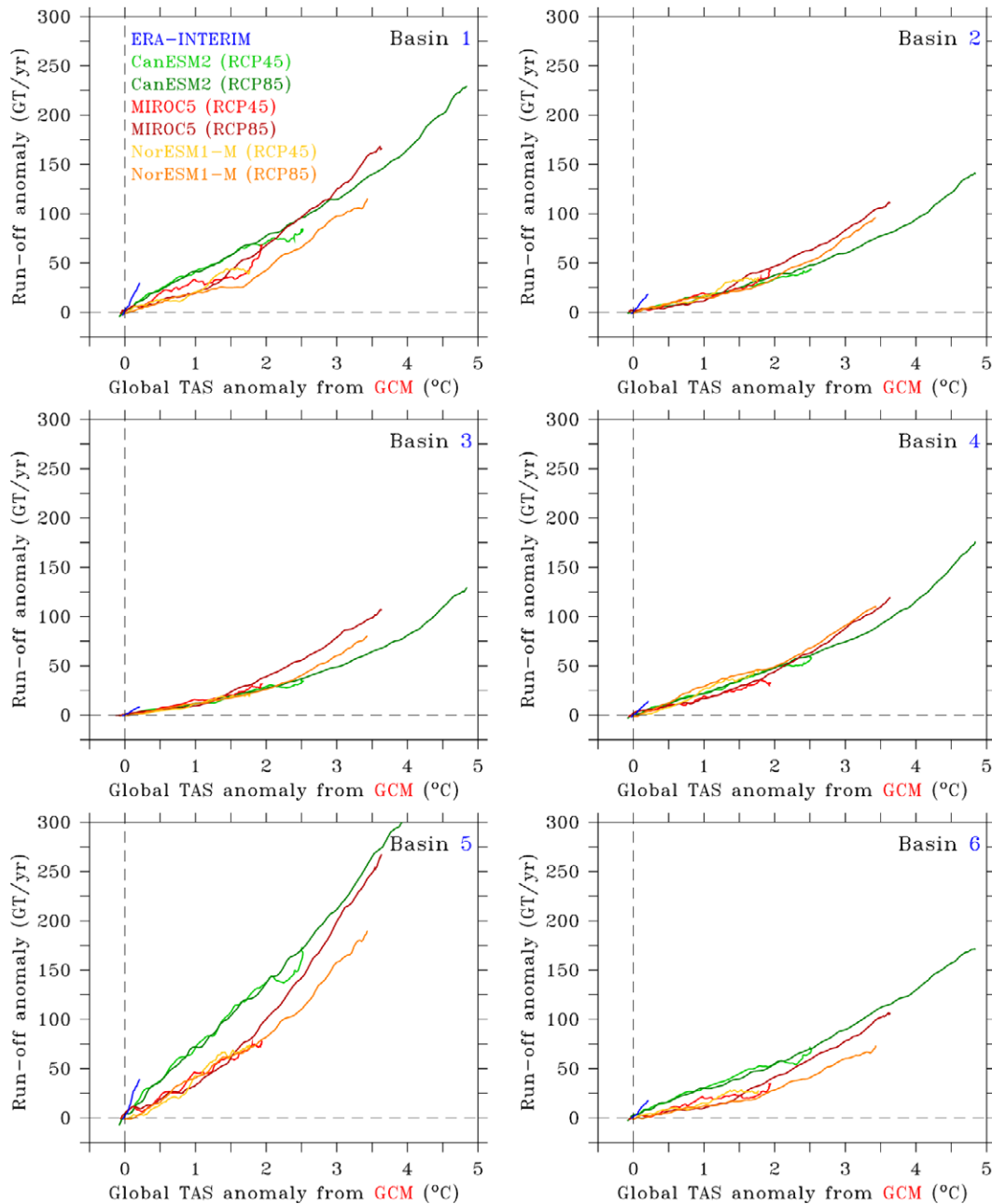


**Figure 4.** Same as figure 2 but for the runoff anomaly.

becomes lower than  $SMB_{ERA_{1980-1999}}$  (i.e. when the SMB in absolute value becomes negative with respect to the ERA-INTERIM forced MAR simulation) and report in table 4 the corresponding globally annual-averaged surface temperature anomaly simulated by the ESMs. All simulations indicate that projected SMB anomaly values for both Basins 1 and 5 will be lower than  $SMB_{ERA_{1980-1999}}$  before the end of this century. In the case of Basin 1, the TAS anomaly values corresponding to the condition when SMB falls below  $SMB_{ERA_{1980-1999}}$  range between  $+0.60$  and  $+1.90$  °C. In the case of Basin 5 the TAS anomaly values range between  $+0.67$  and  $+2.16$  °C, depending on whether MAR projects a strong increase of solid precipitation (NorESM1)

or not (CanESM2 and MIROC5). In the case of Basin 6, four simulations indicate that the SMB will be below the historical mean from  $SMB_{ERA_{1980-1999}}$  (with a near-surface temperature range of  $+1.50$  to  $+3.40$  °C) where only three simulations satisfy the same condition for Basin 2. For the remaining basins there are only two simulations projecting a SMB below the historical MAR-ERA-INTERIM average in the case of Basin 2. This never occurs in the case of Basin 3.

#### 4. Conclusions

The results of the MAR regional climate model forced with the outputs of ESMs obtained in the case of two



**Table 4.** Values of mean global-surface temperature anomaly (1980–99 baseline) corresponding to the condition when the annual projected SMB value is below the 1980–99 mean SMB obtained from MAR forced with ERA-INTERIM. Empty cells indicate that the condition was not met during the study period.

Basin	GCM TAS negative SMB scenario (°C)					
	NorESM1-RCP45	NorESM1-RCP85	CanESM2-RCP45	CanESM2-RCP85	MIROC5-RCP45	MIROC5-RCP85
1	1.21	1.90	0.64	0.60	0.70	1.21
2		2.70		3.18		2.20
3						
4				4.11		3.50
5	1.76	2.16	0.67	0.92	1.64	1.68
6		3.40	1.50	1.89		2.25

greenhouse gases scenarios indicate a regional variability of projected SMB and regional-surface temperature anomalies over Greenland, confirming the importance of studying such quantities at higher spatial resolution than the one achieved with current GCMs. The projected increase of surface temperatures over the Arctic region by the end of this century favours both an increase in runoff (because of increased surface melting) and precipitation (because of increased atmospheric moisture content). Our results indicate that the increase in runoff will exceed the increase in precipitation for all drainage basins, pointing towards negative trends for modelled SMB at all basins.

Basins 1 (north) and 5 (southwest) are the most sensitive, in terms of SMB, to the projected increase of temperature over the 21st century. The advection of warm air in Basin 5 and the projected disappearance of sea ice during the 21st century are likely the major drivers for the increased sensitivity of such basins to a warming scenario. The range for the global TAS anomaly for these two basins to shift to a SMB below the 1980–99 modelled mean value (when the ice sheet was near the equilibrium) is +0.60 to +2.16 °C, depending on the model and scenario. Above those values, the SMB for those basins will be below the equilibrium, potentially moving towards negative SMB absolute annual values. Basin 3 is the only basin where no simulation indicates that SMB will become below the 1980–99 SMB mean simulated by MAR when forced with ERA-INTERIM.

Our results generally point to the fact that higher-surface temperature anomalies are needed to have negative SMB over the eastern basins with respect to the western ones and that the western part of the ice sheet will be in imbalance sooner than the eastern part. This will potentially impact ice sheet dynamics and topography and highlights the necessity of coupling MAR with an ice sheet model. Indeed, due to the absence of this coupling in the simulations reported in this study, the estimated runoff by MAR is not distributed horizontally among the different cells. Moreover, because the ice sheet topography is kept fixed in MAR, the feedback arising from changes in elevation is not accounted for in the current version of the model. Beside impacting melting and runoff through the elevation feedback mechanism, changes in the topography can also impact the surface routing of water and streams distribution, which in turn can impact ice dynamics (e.g., Das *et al* 2008 and Tedesco *et al* 2012b). Increased meltwater production at higher elevations can

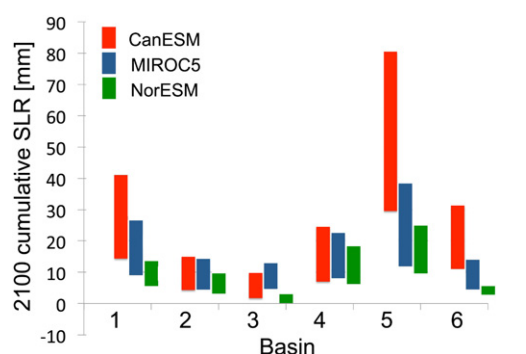


**Figure 5.** 2100 cumulated sea level rise for the different basins obtained from the different scenarios. Top and bottom values in the boxplots represent the values obtained, respectively, with RCP45 (bottom) and RCP85 (top) scenarios.

impact the formation and evolution of supraglacial lakes, especially in the southwest region (Basin 5) of Greenland (where such lakes are more abundant), increasing the potential that the lake population will extend to higher elevations over the summer (Liang *et al* 2012). These lakes will, in turn, trigger other positive feedback mechanisms which will enhance melting or mass loss, impact ice dynamics, reduce surface albedo (because of the increased surface covered by darker water) and increase the ice ablation rate (Tedesco *et al* 2012a). Because our results do not account for the ice sheet topography changes and for ice dynamics, it is plausible to assume that they are conservative with respect to the projected surface mass loss.

Understanding the uncertainty associated with the results of different ESMs to projected increase in CO<sub>2</sub> is a crucial step to obtain improved estimates of SMB changes at a high spatial resolution. The results obtained in this study indicate that the projected cumulative SMB values from each basin translated into a cumulative contribution to sea level rise (in mm) by the end of this century (figure 5) can be up to ~8 cm for Basin 5, and up to ~4 cm for Basin 1. We remark again here that these values do not account for ice dynamics, for the routing of surface water and for changes in elevation. While it is fundamental to continue evaluating the outputs of regional models when forced with outputs from multiple ESMs that have not been considered in this study, it is also important to move in the direction of coupling the regional models with ice

sheet hydrology and ice dynamic models, with the overall goal of reducing the uncertainty associated with the projection of future trends of the total mass balance over the different basins of the Greenland ice sheet.

## Acknowledgments

This work was supported by the NSF grant ARC 0909388. The authors acknowledge the climate modelling groups, the World Climate Research Programme's (WCRP) Working Group on Coupled Modelling (WGCM), and the Global Organization for Earth System Science Portals (GO-ESSP) for their role in producing, coordinating and providing the CMIP5 model outputs.

## References

- Abdalati W and Steffen K 2001 Greenland ice sheet melt extent: 1979–1999 *J. Geophys. Res.* **106** 33983–8
- Alley R B and Joughin I 2012 Modeling ice-sheet flow *Science* **336** 551–2
- Arora V K and Boer G J 2010 Uncertainties in the 20th century carbon budget associated with land use change *Glob. Change Biol.* **16** 3327–48
- Box J E, Bromwich D H and Bai L-S 2004 Greenland ice sheet surface mass balance 1991–2000: application of polar MM5 mesoscale model and *in situ* data *J. Geophys. Res.* **109** D16105
- Box J E, Fettweis X, Stroeve J C, Tedesco M, Hall D K and Steffen K 2012 Greenland ice sheet albedo feedback: thermodynamics and atmospheric drivers *Cryos. Discuss.* **6** 593–634
- Brun E, David P, Sudul M and Brunot G 1992 A numerical model to simulate snowcover stratigraphy for operational avalanche forecasting *J. Glaciol.* **38** 13–22
- Chylek P, Li J, Dubey M K, Wang M and Lesins G 2011 Observed and model simulated 20th century Arctic temperature variability: Canadian earth system model CanESM2 *Atmos. Chem. Phys. Discuss.* **11** 22893–907
- Comiso J C 2002 A rapidly declining perennial sea ice cover in the Arctic *Geophys. Res. Lett.* **29** 1956
- Das S B, Joughin I, Behn M D, Howat I M, King M A, Lizarralde D and Bhatia M P 2008 Fracture propagation to the base of the Greenland ice sheet during supraglacial lake drainage *Science* **320** 778–81
- Fettweis X, Franco B, Tedesco M, van Angelen J H, Lenaerts J T M, van den Broeke M R and Gallée H 2012 Estimating Greenland ice sheet surface mass balance contribution to future sea level rise using the regional atmospheric climate model MAR *Cryos. Discuss.* **6** 3101–47
- Fettweis X, Gallée H, Lefebvre F and van Ypersele J-P 2005 Greenland surface mass balance simulated by a regional climate model and comparison with satellite derived data in 1990–1991 *Clim. Dyn.* **24** 623–40
- Fettweis X, Tedesco M, van den Broeke M and Ettema J 2011 Melting trends over the Greenland ice sheet (1958–2009) from spaceborne microwave data and regional climate models *Cryosphere* **5** 359–75
- Franco B, Fettweis X and Erpicum M 2012 Future projections of the Greenland ice sheet energy balance driving the surface melt, developed using the regional climate MAR model *Cryos. Discuss.* **6** 2265–303
- Helsen M M, van de Wal R S W, van den Broeke M R, van de Berg W J and Oerlemans J 2012 Coupling of climate models and ice sheet models by surface mass balance gradients: application to the Greenland ice sheet *Cryosphere* **6** 255–72
- Krabill W, Abdalati W, Frederick E, Manizade S, Martin C, Sonntag J, Swift R, Thomas R, Wright W and Yungel J 2000 Greenland ice sheet: high-elevation balance and peripheral thinning *Science* **289** 428–30
- Lefebvre F, Fettweis X, Gallée H, van Ypersele J, Marbaix P, Greuell W and Calanca P 2005 Evaluation of a high-resolution regional climate simulation over Greenland *Clim. Dyn.* **25** 99–116
- Lemke P, Ren J, Alley R B, Allison I, Carrasco J, Flato G, Fujii Y, Kaser G, Mote P, Thomas R H and Zhang T 2007 Observations: changes in snow, ice and frozen ground *Climate Change 2007: The Physical Science Basis. Contribution of Working Group I to the Fourth Assessment Report of the Intergovernmental Panel on Climate Change*; ed S Solomon, D Qin, M Manning, Z Chen, M Marquis, K B Avery, M Tignor and H L Miller (Cambridge: Cambridge University Press)
- Liang Y-L, Colgan W, Lv Q, Steffen K, Abdalati W, Stroeve J and Gallaher D 2012 A decadal investigation of supraglacial lakes in West Greenland using a fully automatic detection and tracking algorithm *Remote Sens. Environ.* **123** 127–38
- Meinshausen M, Smith S J, Calvin K, Daniel J S and Kainuma M L T *et al* 2011 The RCP greenhouse gas concentrations and their extensions from 1765 to 2300 *Clim. Change* **109** 213–41
- Moss R H *et al* 2010 The next generation of scenarios for climate change research and assessment *Nature* **463** 747–56
- Rignot E, Braaten D, Gogineni S P, Krabill W B and McConnell J R 2004 Rapid ice discharge from southeast Greenland glaciers *Geophys. Res. Lett.* **31** L10401
- Rignot E, Velicogna I, van den Broeke M R, Monaghan A and Lenaerts J 2011 Acceleration of the contribution of the Greenland and Antarctic ice sheets to sea level rise *Geophys. Res. Lett.* **38** L05503
- Seland O, Iversen T, Kirkevåg A and Storelvmo T 2008 Aerosol–climate interactions in the CAM-Oslo atmospheric GCM and investigation of associated basic shortcomings *Tellus A* **60** 459–91
- Serreze M C, Barrett A P, Stroeve J C, Kindig D N and Holland M M 2009 The emergence of surface-based arctic amplification *Cryosphere* **3** 11–9
- Serreze M C, Walsh J E, Chapin F S III, Osterkamp T, Dyurgerov M B, Romanovsky V, Oechel W C, Morison J, Zhang T and Barry R G 2000 Observational evidence? of recent change in the northern high-latitude environment *Clim. Change* **46** 159–207
- Tedesco M 2007 Snowmelt detection over the Greenland ice sheet from SSM/I brightness temperature daily variations *Geophys. Res. Lett.* **34** L02504
- Tedesco M, Fettweis X, van den Broeke M R, van de Wal R S W, Smeets C J P P, van de Berg W J, Serreze M C and Box J E 2011 The role of albedo and accumulation in the 2010 melting record in Greenland *Environ. Res. Lett.* **6** 014005
- Tedesco M, Luthje M, Steffen K, Steiner N, Fettweis X, Willis I, Bayou N and Banwell A 2012a Measurement and modeling of ablation of the bottom of supraglacial lakes in western Greenland *Geophys. Res. Lett.* **39** L02502
- Tedesco M, Serreze M and Fettweis X 2008 Diagnosing the extreme surface melt event over southwestern Greenland in 2007 *Cryosphere* **2** 159–66

- Tedesco M, Willis I, Hoffman M, Banwell A and Alexander P 2012b Ice dynamic response to slow and fast surface lake drainage on the Greenland ice sheet *Nature Geosci.* submitted
- Thomas R, Csatho B, Davis C, Kim C, Krabill W, Manizade S, McConnell J and Sonntag J 2001 Mass balance of higher-elevation parts of the Greenland ice sheet *J. Geophys. Res.* **106** 33707
- Thomas R, Frederick E, Krabill W, Manizade S and Martin C 2006 Progressive increase in ice loss from Greenland *Geophys. Res. Lett.* **33** L10503
- Vaughan D G and Doake C S M 1996 Recent atmospheric warming and retreat of ice shelves on the Antarctic Peninsula *Nature* **379** 328–30
- Watanabe S *et al* 2010 Improved climate simulation by MIROC5: mean states, variability, and climate sensitivity *J. Clim.* **23** 6312–35
- Watanabe S *et al* 2011 MIROC-ESM: model description and basic results of CMIP5-20c3m experiments *Geosci. Model Dev. Discuss.* **4** 1063–128